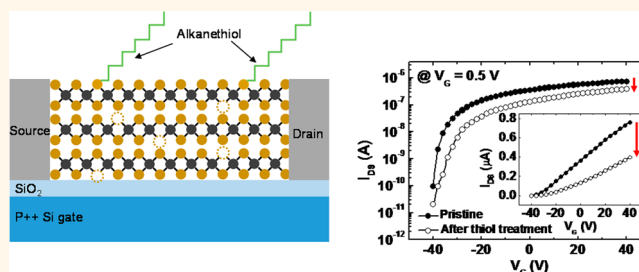


Electrical and Optical Characterization of MoS₂ with Sulfur Vacancy Passivation by Treatment with Alkanethiol Molecules

Kyungjune Cho,[†] Misook Min,[†] Tae-Young Kim,[†] Hyunhak Jeong,[†] Jinsu Pak,[†] Jae-Keun Kim,[†] Jingon Jang,[†] Seok Joon Yun,[‡] Young Hee Lee,[‡] Woong-Ki Hong,[§] and Takhee Lee^{*,†}

[†]Department of Physics and Astronomy and Institute of Applied Physics, Seoul National University, Seoul 151-744, Korea, [‡]IBS Center for Integrated Nanostructure Physics, Institute for Basic Science, Sungkyunkwan University, Suwon 440-746, Korea, and [§]Jeonju Center, Korea Basic Science Institute, Jeonju, Jeollabuk-do 561-180, Korea

ABSTRACT We investigated the physical properties of molybdenum disulfide (MoS₂) atomic crystals with a sulfur vacancy passivation after treatment with alkanethiol molecules including their electrical, Raman, and photoluminescence (PL) characteristics. MoS₂, one of the transition metal dichalcogenide materials, is a promising two-dimensional semiconductor material with good physical properties. It is known that sulfur vacancies exist in MoS₂, resulting in the n-type behavior of MoS₂. The sulfur vacancies on the MoS₂ surface tend to form covalent bonds with sulfur-containing groups. In this study, we deposited alkanethiol molecules on MoS₂ field effect transistors (FETs) and then characterized the electrical properties of the devices before and after the alkanethiol treatment. We observed that the electrical characteristics of MoS₂ FETs dramatically changed after the alkanethiol treatment. We also observed that the Raman and PL spectra of MoS₂ films changed after the alkanethiol treatment. These effects are attributed to the thiol (–SH) end groups in alkanethiols bonding at sulfur vacancy sites, thus altering the physical properties of the MoS₂. This study will help us better understand the electrical and optical properties of MoS₂ and suggest a way of tailoring the properties of MoS₂ by passivating a sulfur vacancy with thiol molecules.



KEYWORDS: molybdenum disulfide · field effect transistor · electronic transport · molecule adsorption

Recently, transition metal dichalcogenide (TMD) two-dimensional (2D) atomic layered materials have drawn considerable attention as promising semiconductors for future ultrathin layered nanoelectronic device applications.^{1,2} Although graphene has several favorable features for use as a 2D layered material, such as high carrier mobility, transparency, and good mechanical properties, graphene has an obvious limitation for use as a semiconductor-active channel because of the absence of an energy band gap.^{3–5} Unlike graphene, TMD materials have a semiconductor band gap with advantages, such as availability of complex device structures with semiconductor properties, good flexibility, and high transparency.^{6,7} Molybdenum disulfide, a member of the TMD family, has been widely

studied due to these advantages. MoS₂ is known to have a direct band gap of ~1.9 eV as a single MoS₂ layer and an indirect band gap of ~1.2 eV as a bulk MoS₂ crystal.^{8,9} Single-layer MoS₂ also has a good carrier mobility (~tens of cm²/(V s) or more) and a high current on/off ratio (~10⁵ or more).^{10–18} Like graphene, MoS₂ flakes with a thickness of a single layer or multiple layers can be prepared by a mechanical exfoliation method using Scotch tape due to a weak van der Waals interaction between MoS₂ layers.⁶ Additionally, large-area MoS₂ films can be synthesized by chemical vapor deposition or by other methods.^{19–21}

One of the potential candidates is the sulfur vacancies of MoS₂.^{22,23} MoS₂ has sulfur vacancies that are considered as the cause of n-type behavior of MoS₂.²² The sulfur

* Address correspondence to tlee@snu.ac.kr.

Received for review March 18, 2015 and accepted August 11, 2015.

Published online August 11, 2015
10.1021/acsnano.5b04400

© 2015 American Chemical Society

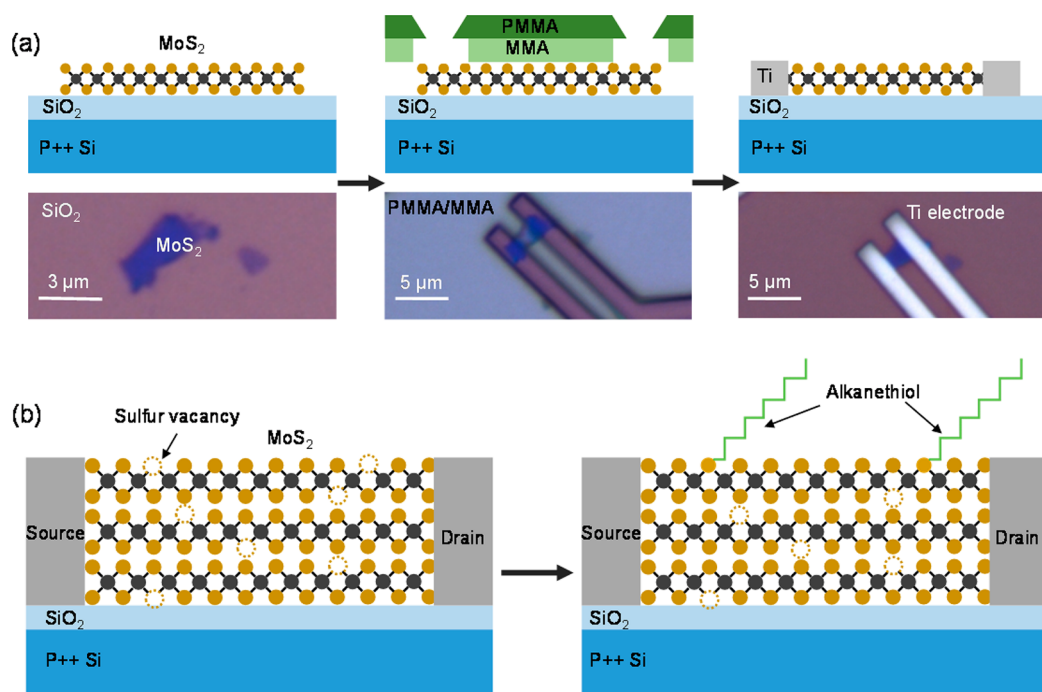


Figure 1. (a) Schematic images of the fabrication process of MoS₂ FETs with the optical images shown under each schematic image. (b) Schematic images of a MoS₂ FET before (left) and after (right) the alkanethiol molecule treatment.

vacancy sites, unsaturated Mo on the surface of MoS₂, have a tendency to covalently bond with sulfur-containing groups.^{24–26} Because of this, MoS₂ has been used as a dehydrosulfurization catalyst; that is, the sulfur vacancies on the basal plane of MoS₂ act as catalytic reaction sites.^{24–26} Therefore, molecules with thiol (–SH) functional groups will form a chemisorbed bond with MoS₂ at the sulfur vacancy positions. Makarova *et al.* have examined the adsorption of thiol molecules with scanning tunneling microscopy, and they indeed observed selective adsorption of thiol molecules at sulfur vacancies on the basal plane of MoS₂.²⁴ If the sulfur vacancies are important for the n-type characteristics of MoS₂ when it is used as a semiconductor device, then the treatment of thiol molecules on MoS₂ would be able to alter the electrical properties of MoS₂ by passivating sulfur vacancies of MoS₂ with thiol molecules.

In this study, we have investigated how the adsorption of thiol molecules on MoS₂ influences the physical and electrical properties of MoS₂. For this purpose, we deposited alkanethiol (HS(CH₂)_{*n*–1}CH₃) molecules on MoS₂ surfaces. Alkanethiols are one of the most widely studied thiol molecules in molecular-based electronic devices.^{27–32} We studied and compared the electrical characteristics of field effect transistors made with exfoliated MoS₂ flakes prior to and after alkanethiol treatment. We also studied and systematically compared the Raman and photoluminescence spectra of exfoliated MoS₂ flakes prior to and after treatment with alkanethiols.

RESULTS AND DISCUSSION

Figure 1a illustrates the fabrication process for MoS₂ field effect transistor (FET) devices. The upper and lower panels in Figure 1a show the schematics and optical microscopic images of a sample during fabrication of the device. First, we prepared the MoS₂ flakes by micromechanical exfoliation from a bulk MoS₂ crystal. The exfoliated MoS₂ flakes were transferred to a 270 nm thick SiO₂ layer on a heavily doped p++ Si substrate, which can be used as a back gate in FET devices (Figure 1a, left). We found appropriate flakes of transferred MoS₂ that can be used for fabrication of FET devices using an optical microscope, and we measured the height of the MoS₂ flakes using an atomic force microscope (AFM). Next, we used an electron beam lithography system to make the source and drain electrode patterns of the FET devices. Here, to prepare well-defined electrode patterns, we used double layers of resists: an electron resist polymer and a buffer layer polymer (Figure 1a, middle). Then, 50 nm thick Ti was deposited as the source and drain electrodes using an electron beam evaporator (Figure 1a, right). Detailed information on the device fabrication is explained in the Methods section and the Supporting Information (Figure S1).

After we fabricated the MoS₂ flake devices, we deposited alkanethiol molecules on the fabricated devices. As explained previously, the thiol molecules tend to form a chemisorbed bond with MoS₂ at the sulfur vacancy positions. Figure 1b shows the schematic

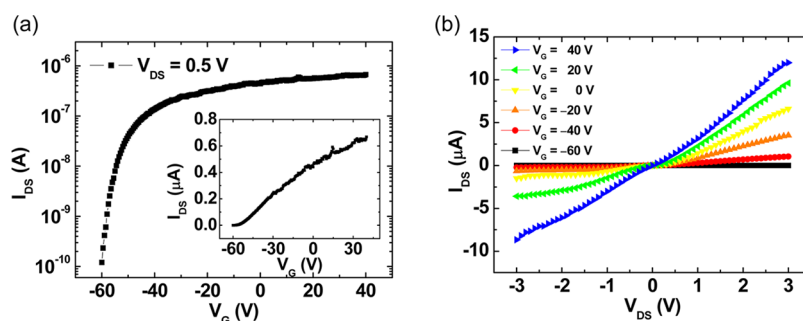


Figure 2. (a) I_{DS} – V_G curve measured at a fixed $V_{DS} = 0.5$ V with logarithmic scale. The inset shows I_{DS} – V_G curves with linear scale. (b) I_{DS} – V_{DS} curves measured with V_G varying from 40 to -60 V.

images of a MoS₂ FET device before and after the alkanethiol treatment. We placed MoS₂ FET devices in the alkanethiol solution for 15 h to allow alkanethiol molecules to be adsorbed on the MoS₂ surface. We characterized and compared the electrical properties of the fabricated MoS₂ FET devices before and after the alkanethiol treatment to examine the effect of alkanethiol absorption on the MoS₂ FET devices. The electrical characterization was performed using a semiconductor parameter analyzer in a probe station. We also systematically characterized some of the transferred MoS₂ flakes (not a FET device structure) on SiO₂/Si substrates prior to and after the alkanethiol treatment process with Raman spectroscopy and photoluminescence. Note that in the study of MoS₂ FET devices, we did not use Au as the electrode because alkanethiol molecules can form a self-assembled monolayer (SAM) on a Au surface. Furthermore, SAM-modified Au electrodes may change the Fermi level of the electrodes and thus cause unwanted source–drain current changes, which may complicate the analysis.

We first measured the basic electrical characteristics of the MoS₂ FET devices prior to the alkanethiol treatment. Figure 2a shows the transfer curve (source–drain current *versus* gate voltage, I_{DS} – V_G) of a MoS₂ FET device measured at a fixed source–drain voltage ($V_{DS} = 0.5$ V) on a logarithmic scale for the source–drain current. The same transfer curve is plotted on the linear scale for the current in the inset of Figure 2a. Figure 2b displays the output curves (source–drain current *versus* source–drain voltage, I_{DS} – V_{DS}) of the device measured with gate voltages varying from 40 to -60 V with steps of 20 V. All of the electrical data were measured in a vacuum ($\sim 10^{-4}$ Torr) to avoid unwanted effects from the ambient environment, such as those from water and oxygen. MoS₂ FET devices may suffer from environmental effects.^{33,34} One thing to notice in Figure 2 is that there was no obvious off-state observed. This can be explained by thermally assisted tunneling through a thin Schottky barrier at the Ti/MoS₂ contact.³⁵ The Ti metal has a work function of ~ 4.3 eV, and MoS₂ has a work function in the range 4.6–4.9 eV. However, although the work function of Ti is smaller than that of MoS₂, there is a Schottky barrier formed

between the Ti and MoS₂.^{39–41} When the Schottky barrier is low and its thickness is ultrathin as in the case of Ti/MoS₂, the charges can transport *via* thermionic emission and thermally assisted tunneling conduction mechanisms.³⁵ This is the reason for the absence of an obvious off-state in MoS₂ with Ti contacts at room temperature.

We estimated the mobility using the following formula: $\mu = (dI_{DS}/dV_G) \times [L/(WC_iV_{DS})]$. In this formula, W is the channel width, L is the channel length, and $C_i = (\epsilon_0\epsilon_r)/d \cong 1.3 \times 10^{-4}$ F/m² is the capacitance between the MoS₂ channel and the p++ Si layer per unit area, where ϵ_r is the dielectric constant of SiO₂ (~ 3.9), ϵ_0 is the vacuum permittivity, and d is the thickness of the SiO₂ layer (270 nm). In this study, we fabricated and characterized a total of 10 MoS₂ FET devices that were prepared from mechanically exfoliated MoS₂ flakes and electron beam lithography. The thickness of exfoliated MoS₂ flakes was found to be in a range from 2.1 to 10.9 nm from AFM, which corresponds to a MoS₂ layer number of 3–17 layers. The estimated mobility values of the MoS₂ FET devices fabricated in this study were found to be in a range from 2.5 to 35.2 cm²/(V s). Additionally, we calculated the carrier concentration of the MoS₂ FETs using the formula $n_e = Q/e = C_G|V_G - V_{Th}|/e$, where C_G is the capacitance of the SiO₂ dielectric layer, $e = 1.6 \times 10^{-19}$ C is the elementary charge, and V_{Th} is the threshold voltage of the FET devices. The mobility and carrier concentrations were measured using the same condition of $V_G = 20$ V and $V_{DS} = 0.5$ V. We determined the V_{Th} values as the x-axis intercept from a linear fitting of the transfer curves. Then, the carrier concentrations of the MoS₂ FET devices were found to be in a range from 2.4×10^{12} to 7.1×10^{12} cm⁻². Detailed electrical parameters of the MoS₂ FET devices characterized in this study are summarized in the Supporting Information (Table S1).

After electrical characterization of the MoS₂ FET devices, we deposited hexadecanethiol (HS(CH₂)₁₅CH₃) on the MoS₂ FET devices. For this purpose, we dipped the MoS₂ FET devices in 5 mM hexadecanethiol in ethanol solution for 15 h in a N₂-filled glovebox. Then, we rinsed the devices with ethanol and measured the electrical properties of the hexadecanethiol-treated MoS₂ FET

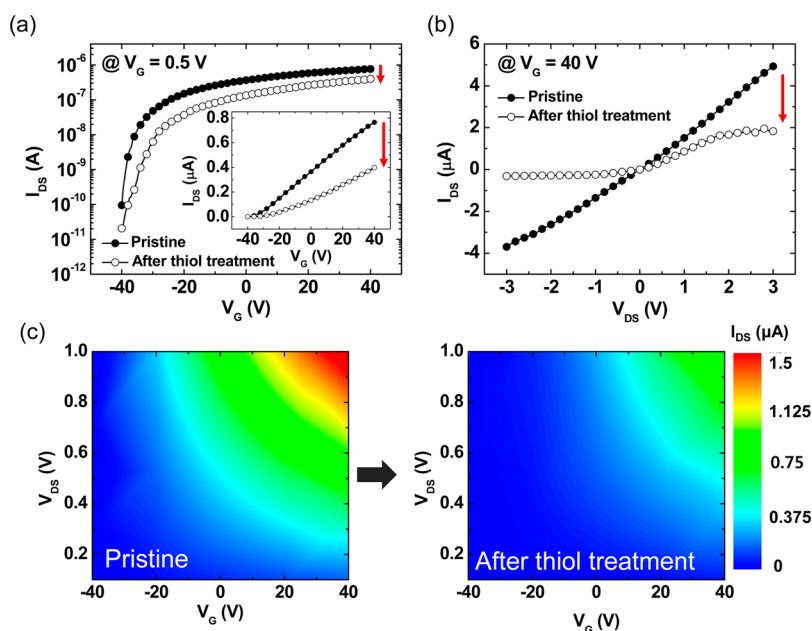


Figure 3. (a) I_{DS} – V_G curves measured before and after the hexadecanethiol treatment with logarithmic scale. The inset shows I_{DS} – V_G curves with linear scale. (b) I_{DS} – V_{DS} curves measured before and after the hexadecanethiol treatment. (c) Contour plots of I_{DS} as a function of V_G and V_{DS} before (left) and after (right) the hexadecanethiol treatment.

devices, again under vacuum conditions. Figure 3a shows the transfer characteristic curves on a logarithmic scale for a MoS₂ FET device. The data represented with filled and open circular symbols are the transfer curves measured before (labeled “Pristine”) and after the hexadecanethiol treatment, respectively. The inset of Figure 3a is the transfer characteristic curves on a linear current scale. The source–drain current level dramatically decreased by ~45%, from 0.58 μA (prior to the molecular treatment) to 0.32 μA (after the molecular treatment) measured at $V_G = 20$ V and $V_{DS} = 0.5$ V. The current decrease can be observed in the output characteristic curves, as shown in Figure 3b. This phenomenon can be more clearly observed in contour plots of the current. Figure 3c displays the contour plots of the source–drain current as a function of V_G and V_{DS} for the MoS₂ FET device that were obtained from the transfer characteristics curves measured for V_{DS} in the range of 0.1 to 1 V and V_G in the range of –40 to 40 V before and after the hexadecanethiol treatment. Here, one can clearly notice that the channel current in the device decreased after the molecular treatment.

The observation of the current decrease phenomenon in MoS₂ FETs after the alkanethiol treatment can be explained in the following manner. Thiol molecules have a sulfur atom at the end group, and the sulfur-containing groups have a tendency to form covalent bonds with unsaturated Mo edges of vacancy defects on the surface of MoS₂.^{24–26} In the vacancy defect sites there are free electrons in unsaturated Mo atoms that do not belong to any chemical bond, and these electrons can behave as charge carriers. However, after the thiol molecule treatment, the thiol molecules are

chemically absorbed at the sulfur vacancy sites on the surface of MoS₂, which decreases the number of free electrons in MoS₂. Also, note that the adsorbed alkanethiol molecules or possible solution residue may behave as defects such as scattering centers, which can also cause additional effects such as the current decrease after the molecule treatment (see Figure S5 in the Supporting Information). The density of the sulfur vacancy has been estimated to be on the order of 10^{13} cm^{-2} from aberration-corrected transmission electron microscopy (TEM) images.²² It is desired to estimate the percentage of sulfur vacancies that are occupied by alkanethiol molecules after the molecule treatment using atomic resolution TEM or other analyses, which is unfortunately beyond the scope of our study.

We consistently observed a similar current decrease phenomena with other MoS₂ FET devices in response to the alkanethiol treatment, and the current contour plots for other MoS₂ FET devices before and after the treatments are provided in the Supporting Information (Figures S2 and S3). To confirm that the reason for the current decrease in the devices is indeed due to the effect of the adsorbed alkanethiol molecules, we treated MoS₂ FET devices in the same way that we processed alkanethiol-treated MoS₂ FET devices but in an ethanol solution that did not contain any alkanethiol molecules. The electrical characterization results for the ethanol-treated devices are shown in the Supporting Information (Figure S5). In this case, the source–drain current of the ethanol-treated MoS₂ FET device did not decrease significantly compared with the case prior to the ethanol treatment. Also notice that the decreased current of alkanethiol-treated MoS₂ FETs

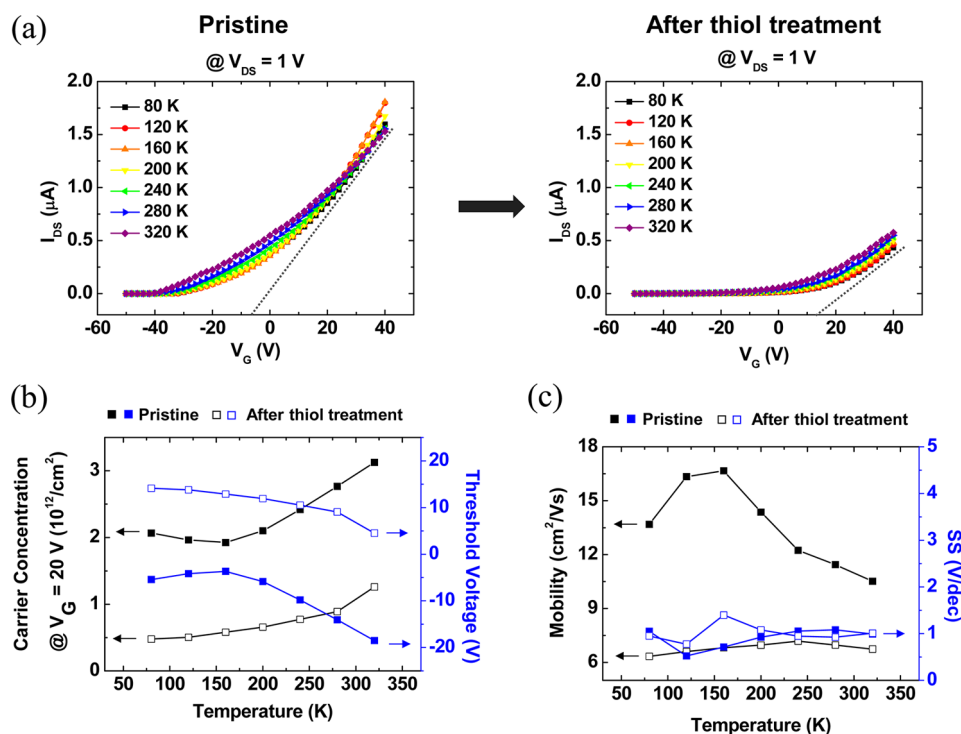


Figure 4. (a) I_{DS} – V_G curves measured before and after hexadecanethiol treatment with varying temperatures from 80 to 320 K. (b) Carrier concentration and threshold voltage of a MoS₂ FET as a function of temperature acquired before and after the hexadecanethiol treatment. (c) Mobility and SS value of a MoS₂ FET as a function of temperature acquired before and after the hexadecanethiol treatment.

recovered the channel current to the value of the pristine condition when we annealed the devices at elevated temperatures over 473 K (see Figure S7 in the Supporting Information).

The current reduction after the thiol molecule treatment can be due to the molecules acting as trap sites or the molecules passivating sulfur vacancies and decreasing the carrier concentration. To find out the dominant mechanism among these, we performed temperature-variable I – V measurements for the devices before and after the alkanethiol molecule treatment. We first measured the V_G – I_{DS} curves of the MoS₂ FET device in the temperature range from 80 to 320 K as shown in the left part of Figure 4a. Then, we treated alkanethiol molecules to the device and measured again; the results are shown in the right part of Figure 4a. From Figure 4a, we can notice that the current level of the device decreased and the threshold voltage shifted in the positive gate voltage direction while the subthreshold swing (SS) value did not change significantly. Figure 4b shows the carrier concentration (black symbols) and threshold voltage (blue symbols) of the device before and after the molecule treatment. Filled and empty square symbols in this figure represent the data that were measured before and after the molecule treatment, respectively. The carrier concentration was estimated at a V_G of 20 V. We can see that the carrier concentration dramatically decreased and the threshold voltage dramatically shifted to the positive

gate voltage direction after the molecule treatment. We also estimated the mobility and SS value of the device, and the results are summarized in Figure 4c. We observed that there was no significant difference in SS values before and after the molecule treatment. The SS value is related with the number of trap sites. If the number of trap sites increases, the SS value would increase. However, the SS value did not change significantly after the molecule treatment, which means that the thiol molecules would not mainly act as trap sites; instead it is more likely that the molecules are passivating sulfur vacancies and decreasing the carrier concentration. In other words, although both the molecules acting as trap sites and the molecules passivating sulfur vacancies and decreasing the carrier concentration can be the reason for the source–drain current reduction, the passivating effect from absorbed alkanethiol molecules seems to be a more dominant effect of the current reduction phenomenon. Furthermore, the SS value did not vary significantly as the temperature was varied. This also supports our interpretation. Note that the mobility of the device decreased after the molecule treatment. This can be explained by a hopping transport model.²² Electrons in the MoS₂ can transport through the sulfur vacancy sites by hopping. With this model, the average distance between the sulfur vacancy sites would increase after the molecule treatment by passivating sulfur vacancy sites of MoS₂. Therefore, it will make the hopping probability decrease and mobility

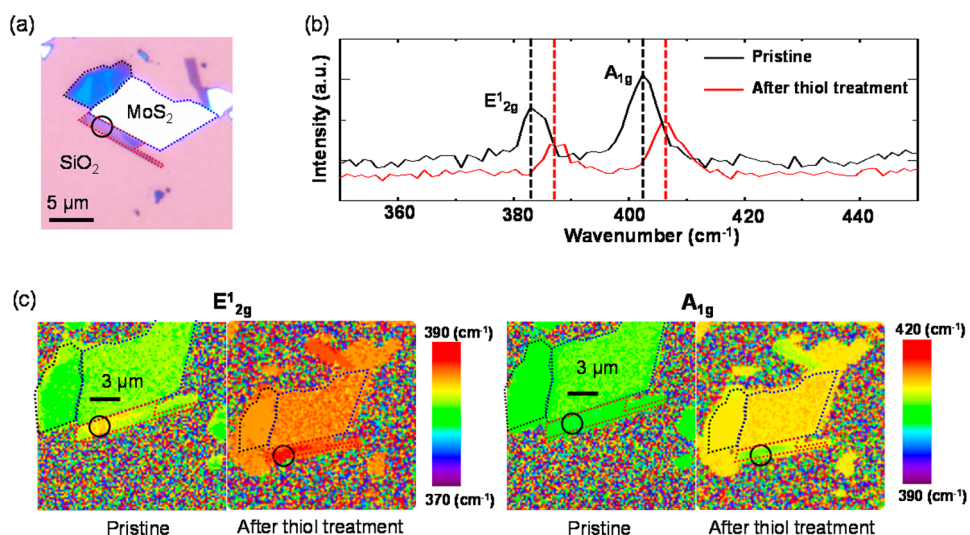


Figure 5. (a) Optical image of a MoS₂ flake that was used for Raman and PL studies. (b) Raman spectra measured from a circled region marked in (a) before and after the hexadecanethiol treatment. (c) Raman mapping image of the E_{12g} mode and A_{1g} mode before (left) and after (right) the hexadecanethiol treatment. We added dotted lines to indicate the MoS₂ flakes in this figure.

decrease as well. Note that if the behavior of the Ti–MoS₂ contact were changed after the molecule treatment, it would change the electrical properties of the devices. However, the contact effect cannot be the dominant reason for our observation. For example, we calculated the effective barrier height with the following formula for a 2D transport channel: $\ln(I_{DS}/T^{3/2}) = -(e/(k_B T))\phi_B + \text{const.}$ ⁴² With this calculation, the effective barrier height was estimated to be changed by ~ 0.03 meV after the molecule treatment (at $V_G = 40$ V), which indicates that the contact effect would not be significant in our study. Also note that the characteristics of contacts between MoS₂ and the Ti electrode are not determined by just comparing Fermi levels of Ti and MoS₂.⁴¹ The sulfur vacancy causes the E_F of MoS₂ to increase, and this result leads to a narrow Schottky barrier for the Ti/MoS₂ contact with a sulfur vacancy.⁴¹ In our case, we treated alkanethiol molecules after the device fabrication. Therefore, the Ti/MoS₂ contact region was already covered by Ti and the alkanethiol molecules were absorbed on the channel only, but not on the Ti/MoS₂ contact region. Besides, the alkanethiol molecules cannot form a self-assembled monolayer on the Ti surface, so molecule treatment does not change the electronic properties of Ti. Therefore, the contact behavior would not be changed before and after the molecule treatment.

If a MoS₂ surface is covered with molecules, then the vibration characteristics of a MoS₂ film will be altered. Because Raman spectroscopy has been used as a powerful tool in studying two-dimensional materials, we measured and compared the Raman spectrum of a MoS₂ flake prior to and after alkanethiol treatment under the same conditions. We used a Raman system with a ~ 1 mW, 532 nm wavelength laser. With the Raman spectroscopic study, one can find

two characteristic normal modes of vibration in MoS₂, an E_{12g} mode and an A_{1g} mode. The E_{12g} peak in the Raman spectrum is the result of in-plane vibrations of Mo atoms and S atoms in opposite directions, and the A_{1g} mode is associated with the S atoms' out-of-plane vibration in the opposite direction. Figure 5a shows the optical image of a MoS₂ flake. We can approximately determine the thickness of the MoS₂ flake from the contrast of the optical image. The black-circled region in Figure 5a is a single-layer MoS₂ flake piece. Figure 5b shows the Raman spectra of a single-layer MoS₂ flake before and after hexadecanethiol treatment. The black and red curves in Figure 5b were measured before and after the hexadecanethiol treatment, respectively. In the case of pristine MoS₂ flakes, *i.e.*, MoS₂ flakes prior to the hexadecanethiol treatment, E_{12g} and A_{1g} modes were observed at 383.0 and 402.3 cm⁻¹, respectively, which suggests that the circled region is indeed a single-layer MoS₂ flake (the difference of the E_{12g} and A_{1g} peak positions is 19.3 cm⁻¹).³⁶ An important finding is that both E_{12g} and A_{1g} modes shifted to a higher wavenumber (blue-shifted). The E_{12g} mode blue-shifted from 383.0 cm⁻¹ to 387.6 cm⁻¹ and the A_{1g} mode blue-shifted from 402.3 cm⁻¹ to 406.9 cm⁻¹. The blue-shift of the E_{12g} and A_{1g} modes can be explained by the molecule adsorption. The chemically absorbed alkanethiol molecules on the MoS₂ surfaces slightly suppress atomic vibrations and lead to a higher force constant of vibration, causing the wavenumber blue-shift. Figure 5c displays the Raman spectra mapping around the peak position of the E_{12g} and A_{1g} modes. In this figure, we added dotted lines to indicate the MoS₂ flakes. After the alkanethiol treatment, the peak positions for both the E_{12g} and A_{1g} modes in every part of the MoS₂ flakes shifted in the direction of higher wavenumbers. We also investigated the effect of another

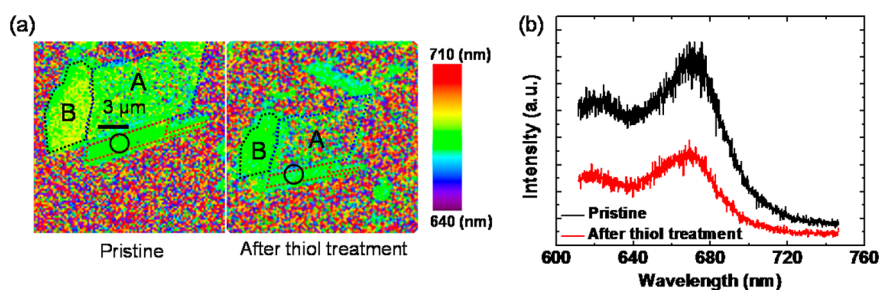


Figure 6. (a) PL peak position mapping image of the MoS₂ flake shown in Figure 4a before (left) and after (right) the hexadecanethiol treatment. (b) PL spectra measured from a circled region before and after the hexadecanethiol treatment. We added dotted lines to indicate the MoS₂ flakes in this figure.

alkanethiol molecule, octanethiol (HS(CH₂)₇CH₃), on MoS₂ by comparing the Raman spectra mapping images of MoS₂ flakes before and after treatment with octanethiol. The results demonstrated that a blue-shift in the Raman data was consistently observed in this case as well (see Figure S9 in the Supporting Information), which suggests that the changed effect is due to the sulfur-containing thiol molecules. Note that the Raman spectra of the MoS₂ flakes did not change noticeably when they were treated with only ethanol solution that did not contain alkanethiol molecules. Furthermore, when we continued to deposit alkanethiols on the MoS₂ flakes that had been treated with ethanol, we consistently observed the blue-shift phenomenon in the Raman spectra (see Figure S9 in the Supporting Information). All these observations suggest that the alkanethiol molecules are the main reason for the blue-shift in the Raman data of the MoS₂ flakes and for the changes in the electrical parameters in the MoS₂ FETs.

In addition to Raman spectroscopy, we also measured the photoluminescence (PL) spectra of MoS₂ before and after the hexadecanethiol treatment. Notice that MoS₂ can be affected by the incident laser's polarization of PL, known as a valley polarization phenomenon in MoS₂,³⁷ and we did not use any polarization filter in order to prevent unwanted effects from the valley polarization. Figure 6a shows the PL mapping image of pristine MoS₂ flakes (left image) and hexadecanethiol-treated MoS₂ flakes (right image). Figure 6b displays the PL spectra that were acquired from the circled regions shown in Figure 6a. Generally, two resonance peaks can be observed in the PL spectra of MoS₂ flakes at ~625 and ~670 nm, which are due to the spin–orbital splitting of the valence band and direct excitonic transitions in MoS₂, respectively.³⁸ We observed that with the hexadecanethiol treatment the PL peaks shifted slightly from 621 nm to 618 nm and from 673 nm to 668 nm and that the intensity of the PL peak decreased noticeably (Figure 6b). Moreover, the PL peak signals from the interband transition in the bulk MoS₂ flake region (marked with A) disappeared, and those in the multi-layer MoS₂ flake region (marked with B) shifted from a yellow to a green color, *i.e.*, in the smaller wavelength direction (Figure 6a), which indicates that the PL peaks

shifted in a high-energy direction. This phenomenon can be explained as follows: generally the PL peak depends on the energy band structure of materials. In MoS₂, a sulfur vacancy provides an electron donor level within the band gap of MoS₂.²² Now, when we treat the MoS₂ with alkanethiol molecules, the number of donor levels in the band gap of MoS₂ decreases by passivating the sulfur vacancy sites of MoS₂ with the alkanethiol molecules. As a result, the intensity of the PL spectrum decreases and the peak position shifts slightly in the high-energy direction, and note that because the PL peak shift is slight, it can be considered that the band gap of MoS₂ was not changed noticeably by the alkanethiol molecule treatment. As a comparison experiment, we measured the PL spectra on MoS₂ flakes that were treated with ethanol solution without alkanethiol molecules. The result was that the PL spectra of the ethanol-treated MoS₂ flakes did not change noticeably (see Figure S10 in the Supporting Information). Additionally, to further verify chemisorption of alkanethiol molecules on the surface of MoS₂, we measured the binding energy of MoS₂ prior to and after the hexadecanethiol molecule treatment using an X-ray photoelectron spectroscopy (XPS) system. The result was that the XPS characteristic peaks' positions of the MoS₂ shifted after the alkanethiol molecule treatment, which indicates that the chemical environment of the MoS₂ was indeed changed (see Figure S8 in the Supporting Information).

As we discussed above, alkanethiol molecules can be chemically absorbed at the sulfur vacancy sites on the surface of MoS₂, and this is the reason for the current decrease, the threshold voltage shift, the Raman peak shift, and the changes in PL spectra with the treatment with thiol molecules. The number of sulfur vacancy sites depends on the surface area of the MoS₂ channel. Thus, the effect of alkanethiol molecules depends on the surface area of the MoS₂ channel. Additionally, this effect depends on the thickness of the MoS₂ flakes because MoS₂ is a two-dimensional layered material and the height is a major factor in determining the surface to volume ratio of the MoS₂ layer. Figure 7a displays the current difference *versus* height data plot. We measured the channel current for

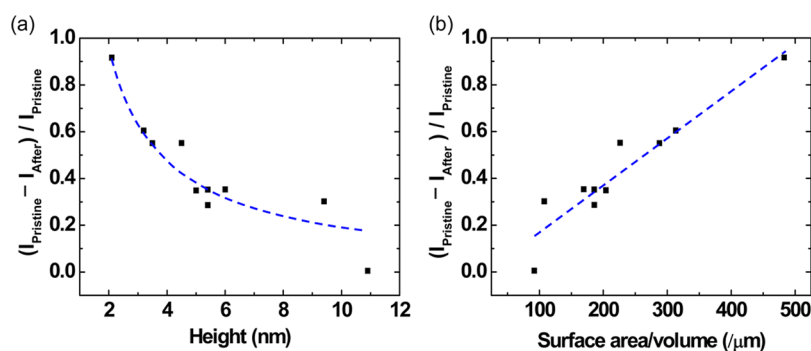


Figure 7. (a) Difference in channel currents measured before (I_{Pristine}) and after (I_{After}) the hexadecanethiol treatment for 10 MoS₂ FET devices with different layer thicknesses (height) of the MoS₂ channel. (b) Difference channel currents before and after hexadecanethiol treatment as a function of the surface area to volume ratio of the MoS₂ channel film. The blue dashed lines were added to demonstrate the dependence of the channel current difference on the MoS₂ channel's height or surface area to volume ratio.

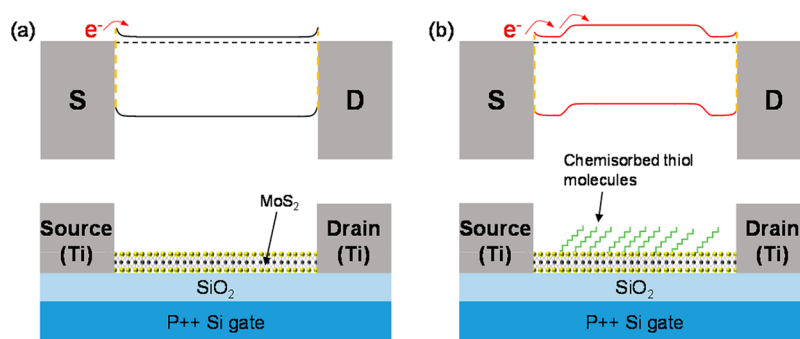


Figure 8. Schematics of the energy band diagram at $V_G = 0$ (a) before and (b) after the alkanethiol molecule treatment.

all the MoS₂ FET devices that we fabricated and calculated the current difference as $(I_{\text{Pristine}} - I_{\text{After}}) / I_{\text{Pristine}}$. Here, I_{Pristine} and I_{After} are the current levels of the devices that were measured at $V_G = 20$ V and $V_{\text{DS}} = 0.5$ V prior to and after the alkanethiol treatment. For this study, we fabricated a total of 10 MoS₂ FET devices that were prepared from mechanically exfoliated MoS₂ flakes, of which the thickness varied from 2 to 11 nm. As can be observed in the plot of Figure 7a, the current difference is proportional to the inverse of the thickness of the MoS₂ channel. The blue dashed curve in this plot was added to show this dependence. Figure 7b displays the plot of the current difference versus the surface area to volume ratio. We calculated the values of surface area to volume ratio as $(2hl + w)/hw$, where h is the thickness of the MoS₂ channel, w is the channel width, and l is the channel length. As shown in Figure 7b, the current difference of the MoS₂ FETs depended on the MoS₂ channel's surface to volume ratio. The results in Figure 6 show that the effect of the alkanethiol adsorption to the MoS₂ surface on the channel current of MoS₂ FETs decreases as the thickness of the MoS₂ channel increases (*i.e.*, the surface area to volume decreases). We also calculated the carrier concentration difference and mobility difference of the characterized MoS₂ FET devices, and the results are provided in the Supporting Information (Figure S6).

We now explain the effect of alkanethiol molecule adsorption on the MoS₂ surface using the energy band diagrams as shown in Figure 8. Figure 8a and b show the energy band diagram before and after the alkanethiol adsorption. The Ti metal as the source–drain electrode has a work function of ~ 4.3 eV, and MoS₂ has a work function in the range 4.6–4.9 eV. However, although the work function of Ti is smaller than that of MoS₂, there is a Schottky barrier formed between the Ti and MoS₂.^{39–41} Figure 8b shows the energy band diagram after the alkanethiol molecule treatment. When the MoS₂ devices are treated with alkanethiol molecules, the alkanethiol molecules that are chemically adsorbed at the surface of MoS₂ can capture the electrons of unsaturated Mo in MoS₂ and deplete the MoS₂ channel. Thus, alkanethiol molecules act as an energy barrier, resulting in the decrease of the channel current (Figure 3).

CONCLUSION

In summary, we fabricated MoS₂ FETs and measured their physical properties before and after alkanethiol molecule treatment to investigate the effect of passivating sulfur vacancy on the surface of MoS₂. After treatment with alkanethiol molecules, we observed that the source–drain current of the MoS₂ FETs decreased dramatically. In addition, the Raman spectrum peaks

(E_{12g} and A_{1g}) of the MoS_2 flakes exhibited a blue-shift, and the PL peaks disappeared or slightly shifted after the alkanethiol treatment. From the temperature-variable electrical characterization, the changes in physical and electrical properties of MoS_2 flakes and MoS_2 FET devices are a result of the alkanethiol

molecules capturing the electrons in MoS_2 by passivating sulfur vacancy sites (unsaturated Mo) on the MoS_2 surface. Our study may foster a way of tailoring the electrical and optical properties of MoS_2 by sulfur vacancy passivation using sulfur-containing molecules.

METHODS

The MoS_2 flakes used in this study were exfoliated using the micromechanical exfoliation method from a bulk MoS_2 crystal purchased from SPI Supplies, USA. Then, the exfoliated MoS_2 flakes were transferred from 3M Scotch tape to SiO_2 on a heavily doped p++ Si wafer (resistivity $\sim 5 \times 10^{-3} \Omega \text{ cm}$), which can be used as a back gate. After finding the location of a multilayer MoS_2 flake using an optical microscope, the MoS_2 flakes' height was measured with an NX 10 AFM system (Park Systems). To make patterns of electrodes, we spin-coated methyl methacrylate (MMA) (8.5) and MMA (9% concentration in ethyl lactate) as a buffer layer and poly(methyl methacrylate) (PMMA) 950 K (5% concentration in anisole) as electron resist at 4000 rpm. After the spin-coating of each layer, the sample was baked at 180 °C for 90 s. The electrodes of MoS_2 FETs were patterned using an electron beam lithography system (JSM-6510, JEOL) with a 30 kV exposure. The pattern development was performed with a methyl isobutyl ketone/isopropyl alcohol (1:3) solution with a development time of 50 s. The electrical characteristics of the device were measured using a semiconductor parameter analyzer (Keithley 4200-SCS) in a probe station (JANIS model ST-500). Also, the Raman and PL characteristics of the MoS_2 flakes were measured using a Raman system (CRM 200, WiTec, Germany).

Conflict of Interest: The authors declare no competing financial interest.

Supporting Information Available: The Supporting Information is available free of charge on the ACS Publications website at DOI: 10.1021/acsnano.5b04400.

The device fabrication, characteristic parameters of MoS_2 FET devices, contour plots of the source–drain currents for other MoS_2 FET devices, electrical data of a MoS_2 FET with ethanol treatment, statistic data of mobility difference and carrier concentration difference, electrical data of alkanethiol-treated MoS_2 FET at elevated temperatures, XPS data of MoS_2 flakes before and after alkanethiol treatment, Raman and PL data with ethanol and octanethiol molecule treatment, as well as supplementary figures and a table (PDF)

Acknowledgment. The authors appreciate financial support from the National Creative Research Laboratory Program (Grant No. 20120226372) of Korea and the National Core Research Center (Grant No. R15-2008-006-03002-0) through the National Research Foundation of Korea, funded by the Korean Ministry of Science, ICT & Future Planning.

REFERENCES AND NOTES

- Novoselov, K.; Geim, A. K.; Morozov, S.; Jiang, D.; Zhang, Y.; Dubonos, S.; Grigorieva, I.; Firsov, A. Electric Field Effect in Atomically Thin Carbon Films. *Science* **2004**, *306*, 666–669.
- Novoselov, K. S.; Jiang, D.; Schedin, F.; Booth, T. J.; Khotkevich, V. V.; Morozov, S. V.; Geim, A. K. Two-Dimensional Atomic Crystals. *Proc. Natl. Acad. Sci. U. S. A.* **2005**, *102*, 10451–10453.
- Li, X.; Wang, X.; Zhang, L.; Lee, S.; Dai, H. Chemically Derived, Ultrasoft Graphene Nanoribbon Semiconductors. *Science* **2008**, *319*, 1229–1232.
- Allen, M. J.; Tung, V. C.; Kanar, R. B. Honeycomb Carbon: A Review of Graphene. *Chem. Rev.* **2010**, *110*, 132–145.
- Xu, Y.; Bai, H.; Lu, G.; Li, C.; Shi, G. Flexible Graphene Films via the Filtration of Water-Soluble Noncovalent Functionalized Graphene Sheets. *J. Am. Chem. Soc.* **2008**, *130*, 5856–5857.
- Radisavljevic, B.; Radenovic, A.; Brivio, J.; Giacometti, V.; Kis, A. Single-Layer MoS_2 Transistors. *Nat. Nanotechnol.* **2011**, *6*, 147–150.
- Fang, H.; Chuang, S.; Chang, T. C.; Takei, K.; Takahashi, T.; Javey, A. High-Performance Single Layered WSe_2 p-FETs with Chemically Doped Contacts. *Nano Lett.* **2012**, *12*, 3788–3792.
- Kam, K.; Parkinson, B. Detailed Photocurrent Spectroscopy of the Semiconducting Group VIB Transition Metal Dichalcogenides. *J. Phys. Chem.* **1982**, *86*, 463–467.
- Mak, K. F.; Lee, C.; Hone, J.; Shan, J.; Heinz, T. F. Atomically Thin MoS_2 : A New Direct-Gap Semiconductor. *Phys. Rev. Lett.* **2010**, *105*, 136805.
- Jariwala, D.; Sangwan, V. K.; Lauhon, L. J.; Marks, T. J.; Hersam, M. C. Emerging Device Applications for Semiconducting Two-Dimensional Transition Metal Dichalcogenides. *ACS Nano* **2014**, *8*, 1102–1120.
- Perkins, F. K.; Friedman, A. L.; Cobas, E.; Campbell, P. M.; Jernigan, G. G.; Jonker, B. T. Chemical Vapor Sensing with Monolayer MoS_2 . *Nano Lett.* **2013**, *13*, 668–673.
- Lee, H. S.; Min, S. W.; Park, M. K.; Lee, Y. T.; Jeon, P. J.; Kim, J. H.; Ryu, S.; Im, S. MoS_2 Nanosheets for Top-Gate Nonvolatile Memory Transistor Channel. *Small* **2012**, *8*, 3111–3115.
- Wang, H.; Yu, L.; Lee, Y. H.; Shi, Y.; Hsu, A.; Chin, M. L.; Li, L. J.; Dubey, M.; Kong, J.; Palacios, T. Integrated Circuits Based on Bilayer MoS_2 Transistors. *Nano Lett.* **2012**, *12*, 4674–4680.
- Yin, Z.; Zeng, Z.; Liu, J.; He, Q.; Chen, P.; Zhang, H. Memory Devices Using a Mixture of MoS_2 and Graphene Oxide as the Active Layer. *Small* **2013**, *9*, 727–731.
- Radisavljevic, B.; Whitwick, M. B.; Kis, A. Integrated Circuits and Logic Operations Based on Single-Layer MoS_2 . *ACS Nano* **2011**, *5*, 9934–9938.
- Choi, W.; Cho, M. Y.; Konar, A.; Lee, J. H.; Cha, G. B.; Hong, S. C.; Kim, S.; Kim, J.; Jena, D.; Joo, J.; et al. High-Detectivity Multilayer MoS_2 Phototransistors with Spectral Response from Ultraviolet to Infrared. *Adv. Mater.* **2012**, *24*, 5832–5836.
- Li, H.; Yin, Z.; He, Q.; Li, H.; Huang, X.; Lu, G.; Fam, D. W. H.; Tok, A. I. Y.; Zhang, Q.; Zhang, H. Fabrication of Single- and Multilayer MoS_2 Film-Based Field-Effect Transistors for Sensing NO at Room Temperature. *Small* **2012**, *8*, 63–67.
- Kim, S.; Konar, A.; Hwang, W. S.; Lee, J. H.; Lee, J.; Yang, J.; Jung, C.; Kim, H.; Yoo, J. B.; Choi, J. Y.; et al. High-Mobility and Low-Power Thin-Film Transistors Based on Multilayer MoS_2 Crystals. *Nat. Commun.* **2012**, *3*, 1011.
- Wu, S.; Huang, C.; Aivazian, G.; Ross, J. S.; Cobden, D. H.; Xu, X. Vapor-Solid Growth of High Optical Quality MoS_2 Monolayers with Near-Unity Valley Polarization. *ACS Nano* **2013**, *7*, 2768–2772.
- Eda, G.; Yamaguchi, H.; Voiry, D.; Fujita, T.; Chen, M.; Chhowalla, M. Photoluminescence from Chemically Exfoliated MoS_2 . *Nano Lett.* **2011**, *11*, 5111–5116.
- Lee, Y. H.; Zhang, X. Q.; Zhang, W.; Chang, M. T.; Lin, C. T.; Chang, K. D.; Yu, Y. C.; Wang, J. T. W.; Chang, C. S.; Li, L. J.; et al. Synthesis of Large-Area MoS_2 Atomic Layers with Chemical Vapor Deposition. *Adv. Mater.* **2012**, *24*, 2320–2325.

22. Qiu, H.; Xu, T.; Wang, Z.; Ren, W.; Nan, H.; Ni, Z.; Chen, Q.; Yuan, S.; Miao, F.; Song, F.; Long, G.; Shi, Y.; Sun, L.; Wang, J.; Wang, X. Hopping Transport through Defect-Induced Localized States in Molybdenum Disulphide. *Nat. Commun.* **2013**, *4*, 2642.
23. Noh, J.-Y.; Kim, H.; Kim, Y.-S. Stability and Electronic Structures of Native Defects in Single-layer MoS₂. *Phys. Rev. B: Condens. Matter Mater. Phys.* **2014**, *89*, 205417.
24. Makarova, M.; Okawa, Y.; Aono, M. Selective Adsorption of Thiol Molecules at Sulfur Vacancies on MoS₂(0001), Followed by Vacancy Repair via S-C Dissociation. *J. Phys. Chem. C* **2012**, *116*, 22411–22416.
25. Wiegenstein, C. G.; Schulz, K. H. Methanethiol Adsorption on Defective MoS₂(0001) Surfaces. *J. Phys. Chem. B* **1999**, *103*, 6913–6918.
26. Peterson, S. L.; Schulz, K. H. Ethanethiol Decomposition Pathways on MoS₂(0001). *Langmuir* **1996**, *12*, 941–945.
27. Cygan, M. T.; Dunbar, T. D.; Arnold, J. J.; Bumm, L. A.; Shedlock, N. F.; Burgin, T. P.; Jones, L. II; Allara, D. L.; Tour, J. M.; Weiss, P. S. Insertion, Conductivity, and Structures of Conjugated Organic Oligomers in Self-Assembled Alkanethiol Monolayers on Au{111}. *J. Am. Chem. Soc.* **1998**, *120*, 2721–2732.
28. Park, S.; Wang, G.; Cho, B.; Kim, Y.; Song, S.; Ji, Y.; Yoon, M. H.; Lee, T. Flexible Molecular-Scale Electronic Devices. *Nat. Nanotechnol.* **2012**, *7*, 438–442.
29. Kumar, A.; Whitesides, G. M. Features of Gold Having Micrometer to Centimeter Dimensions Can be Formed through a Combination of Stamping with an Elastomeric Stamp and an Alkanethiol “Ink” Followed by Chemical Etching. *Appl. Phys. Lett.* **1993**, *63*, 110628.
30. Poirier, G. E.; Tarlov, M. J. The c(4 × 2) Superlattice on n-Alkanethiol Monolayers Self-Assembled on Au(111). *Langmuir* **1994**, *10*, 2853–2856.
31. Reed, M. A.; Zhou, C.; Muller, C. J.; Burgin, T. P.; Tour, J. M. Conductance of a Molecular Junction. *Science* **1997**, *278*, 252–254.
32. Najmaei, S.; Zou, X.; Er, D.; Li, J.; Jin, Z.; Gao, W.; Zhang, Q.; Park, S.; Ge, L.; Lei, S.; Kono, J.; Shenoy, V. B.; Yakobson, B. I.; George, A.; Ajayan, P. M.; Lou, J. Tailoring the Physical Properties of Molybdenum Disulfide Monolayers by Control of Interfacial Chemistry. *Nano Lett.* **2014**, *14*, 1354–1361.
33. Cho, K.; Park, W.; Park, J.; Jeong, H.; Jang, J.; Kim, T. Y.; Hong, W. K.; Hong, S.; Lee, T. Electric Stress-Induced Threshold Voltage Instability of Multilayer MoS₂ Field Effect Transistors. *ACS Nano* **2013**, *7*, 7751–7758.
34. Park, W.; Park, J.; Jang, J.; Lee, H.; Jeong, H.; Cho, K.; Hong, S.; Lee, T. Oxygen Environmental and Passivation Effects on Molybdenum Disulfide Field Effect Transistors. *Nanotechnology* **2013**, *24*, 095202.
35. Das, H.; Chen, H.-Y.; Penumatcha, A. V.; Appenzeller, J. High Performance Multilayer MoS₂ Transistors with Scandium Contacts. *Nano Lett.* **2013**, *13*, 100–105.
36. Li, H.; Zhang, Q.; Yap, C. C. R.; Tay, B. K.; Olivier, T. H. T. E. A.; Baillargeat, D. From Bulk to Monolayer MoS₂; Evolution of Raman Scattering. *Adv. Funct. Mater.* **2012**, *22*, 1385–1390.
37. Zeng, H.; Dai, J.; Yao, W.; Xiao, D.; Cui, X. Valley Polarization in MoS₂ Monolayers by Optical Pumping. *Nat. Nanotechnol.* **2012**, *7*, 490–493.
38. Splendiani, A.; Sun, L.; Zhang, Y.; Li, T.; Kim, J.; Chim, C. Y.; Galli, G.; Wang, F. Emerging Photoluminescence in Monolayer MoS₂. *Nano Lett.* **2010**, *10*, 1271–1275.
39. Feng, L. P.; Su, J.; Liu, Z. T. Effect of Vacancies on Structural, Electronic and Optical Properties of Monolayer MoS₂: A First-Principles Study. *J. Alloys Compd.* **2014**, *613*, 122–127.
40. Kang, J.; Liu, W.; Banerjee, K. High-Performance MoS₂ Transistors with Low-Resistance Molybdenum Contacts. *Appl. Phys. Lett.* **2014**, *104*, 233502.
41. Feng, L. P.; Su, K.; Li, D. P.; Liu, Z. T. Tuning the Electronic Properties of Ti-MoS₂ Contacts Through Introducing Vacancies in Monolayer MoS₂. *Phys. Chem. Chem. Phys.* **2015**, *17*, 6700.
42. Wang, W.; Liu, Y.; Tang, L.; Jin, Y.; Zhao, T.; Xiu, F. Controllable Schottky Barriers between MoS₂ and Permalloy. *Sci. Rep.* **2014**, *4*, 6928.